Palaeogeography, Palaeoclimatology, Palaeoecology 271 (2009) 39–51

Contents lists available at ScienceDirect

Palaeogeography, Palaeoclimatology, Palaeoecology

journal homepage: www.elsevier.com/locate/palaeo

Distribution of clay minerals in Early Jurassic Peritethyan seas: Palaeoclimatic significance inferred from multiproxy comparisons

Guillaume Dera *, Pierre Pellenard, Pascal Neige, Jean-François Deconinck, Emmanuelle Pucéat, Jean-Louis Dommergues

University of Burgundy, Biogéosciences, UMR CNRS 5561, 6 boulevard Gabriel, F-21000 Dijon, France

ARTICLE INFO

Article history:
Received 2 April 2008
Received in revised form 18 August 2008
Accepted 15 September 2008

Keywords:
Clay minerals
Palaeoclimate
Pliensbachian
Toarcian

ABSTRACT

A set of published, unpublished, and new clay mineral data from 60 European and Mediterranean localities allows us to test the reliability of clay minerals as palaeoclimatic proxies for the Pliensbachian–Toarcian period (Early Jurassic) by reconstructing spatial and temporal variations of detrital fluxes at the ammonite biochronozone resolution. In order to discuss their palaeoclimatic meaning, a compilation of low-latitude belemnite $\delta^{18}O$, $\delta^{13}C$, Mg/Ca, and $^{87}Sr/^{86}Sr$ values is presented for the first time for the whole Pliensbachian–Toarcian period. Once diagenetic and authigenic biases have been identified and ruled out, kaolinite content variation is considered as a reliable palaeoclimatic proxy for the Early Jurassic. Major kaolinite enrichments occur during times of low $\delta^{18}O$, high Mg/Ca, and increasing $^{87}Sr/^{86}Sr$, implying warm climates and efficient runoffs during the Davoei, Falciferum and Bifrons Zones. Conversely, cooler and drier times such as the Late Pliensbachian or the Late Toarcian are characterized by low hydrolysis of landmasses, and correspond to kaolinite depleted intervals. Secondary factors as modifications of sources or hydrothermalism may sporadically disturb the palaeoclimatic signal (e.g., in the Bakony area during the Late Pliensbachian). In addition, a spatial comparison of clay assemblages displays significant kaolinite enrichments towards northern parts of the Peritethyan Realm, probably related to the latitudinal zonation of hydrolyzing conditions. This implies enhanced runoffs on northern continental landmasses that reworked kaolinite-rich sediments from subtropical soils and/or Palaeozoic substrata.

1. Introduction

The Pliensbachian–Toarcian interval (189.6–175.6±2 Ma, Gradstein et al., 2004) was a period of dramatic environmental changes. Worldwide deposits of black shales are reported for the Early Toarcian and attributed to a global oceanic anoxic event (OAE) (Jenkyns, 1988) that may have triggered a second order biodiversity crisis (Little and Benton, 1995; Pálfy and Smith, 2000; Cecca and Macchioni, 2004; Wignall et al., 2005). This period is also characterized by significant disruptions in the carbon cycle and by calcification crises (Jenkyns and Clayton, 1997; Tremolada et al., 2005; Hesselbo et al., 2007; Suan et al., 2008a,b), the causes of which are still highly controversial. Current hypotheses include palaeoceanographic disturbances, massive releases of methane gas-hydrates, and greenhouse gas inputs resulting from volcanic activity or metamorphic alterations of Gondwanan coals in the Karoo-Ferrar province (Fig. 1) (Hesselbo et al., 2000a; Schouten et al., 2000; Kemp et al., 2005a; McElwain et al., 2005; Van de Schootbrugge et al., 2005b; Wignall et al., 2006; Svensen et al., 2007).

Recent studies based on $\delta^{18}O$ and Mg/Ca of belemnites and brachiopods have highlighted significant variations of seawater temperatures during this period (McArthur et al., 2000; Bailey et al., 2003; Rosales et al., 2004; Van de Schootbrugge et al., 2005a; Metodiev and Koleva-Rekalova, 2006; Gómez et al., 2008; Suan et al., 2008b). Available data suggest slight warming during the Early Pliensbachian, followed by significant cooling during the Late Pliensbachian, while intense warming events occurred during the Early and Middle Toarcian. However, seawater temperatures derived from belemnite and brachiopod $\delta^{18}O$ values remain controversial owing to large freshwater inputs, chiefly during the Toarcian, that make it difficult to decipher the respective influences of temperature and $\delta^{18}O_{seawater}$ variations in the calcite $\delta^{18}O$ signal (Bailey et al., 2003; Suan et al., 2008b). Thus, combined approaches integrating independent palaeoclimatic proxies, and particularly those reflecting continental contexts, remain essential to improve our knowledge of this major disturbed climatic period.

Clay mineral assemblages act in this context as a useful palaeoclimatic proxy because clay minerals deposited in modern or past marine environments are mainly inherited from landmasses after weathering of primary rocks and pedogenesis (Chamley, 1989). The nature of clay assemblages in modern sediments is closely related to the geodynamic context, to the composition of weathered primary

* Corresponding author. Fax: +33 3 80 39 63 87.
E-mail address: guillaume.dera@u-bourgogne.fr (G. Dera).

0031-0182/$ – see front matter © 2008 Elsevier B.V. All rights reserved.
doi:10.1016/j.palaeo.2008.09.010

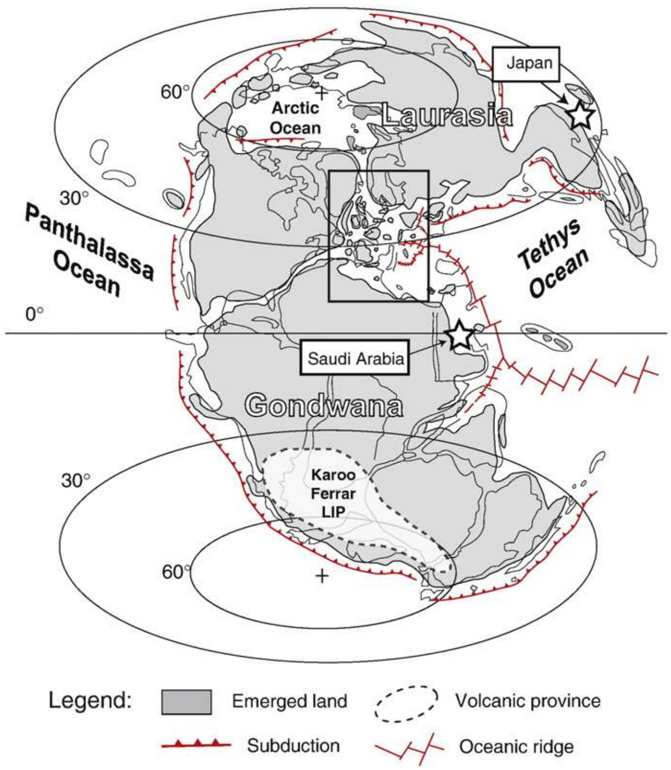

Fig. 1. World palaeogeography during the Early Jurassic (modified from Damborenea, 2002). The Peritethyan realm is framed.

rocks, and to the hydrolysis intensity which varies with climatic conditions (Biscaye, 1965; Singer, 1984; Chamley, 1989). During recent glacial/interglacial alternations, chlorite versus illite proportions in sediments, for example, have been clearly assigned to climatic variations (Vanderaveroet et al., 1999; Bout-Roumazeilles et al., 2007). In old sedimentary series, special care has to be taken because sediment reworking, diagenesis, or authigenesis may transform the primary composition, and alter the palaeoclimatic signal (Thiry, 2000). Nevertheless, once these effects are estimated and discriminated, clay minerals such as kaolinite and/or smectite may be successfully used as indicators of humid versus arid conditions for the Mesozoic period (Ruffell et al., 2002; Pellenard and Deconinck, 2006; Schnyder et al., 2006; Raucsik and Varga, 2008). As clay mineral assemblages depend on local factors, a reliable palaeoclimatic signal can be detected only if the study is conducted at regional scale, using interbasin comparisons for a given period.

In the present study, we test the potential and reliability of clay mineral variation as a palaeoclimatic proxy for the Pliensbachian–Toarcian period. We present an original and sizeable database collating biostratigraphically well-constrained clay mineral data from an extensive literature survey of Peritethyan sections to which we also add some personal clay mineral data. In addition, a compilation of low-latitude belemnite $\delta^{18}O$, $\delta^{13}C$, Mg/Ca, and $^{87}Sr/^{86}Sr$ values is presented for the first time for the whole Pliensbachian–Toarcian period. The distribution of clay species over time and space is then discussed in the context of available geochemical and sedimentological data, and tentatively used to specify climatic changes during the Pliensbachian–Toarcian interval.

2. Material and method

Published and unpublished clay mineral data from the Pliensbachian–Toarcian period have been gathered from 60 localities in 20 European and Mediterranean basins (Fig. 2A). During the Early Jurassic, these basins were epicontinental seas of the Peritethyan Realm (Figs. 1 and 2B). Data from Japan and Saudi Arabia also complete this compilation (Fig. 1). Except for samples from Norwegian Sea

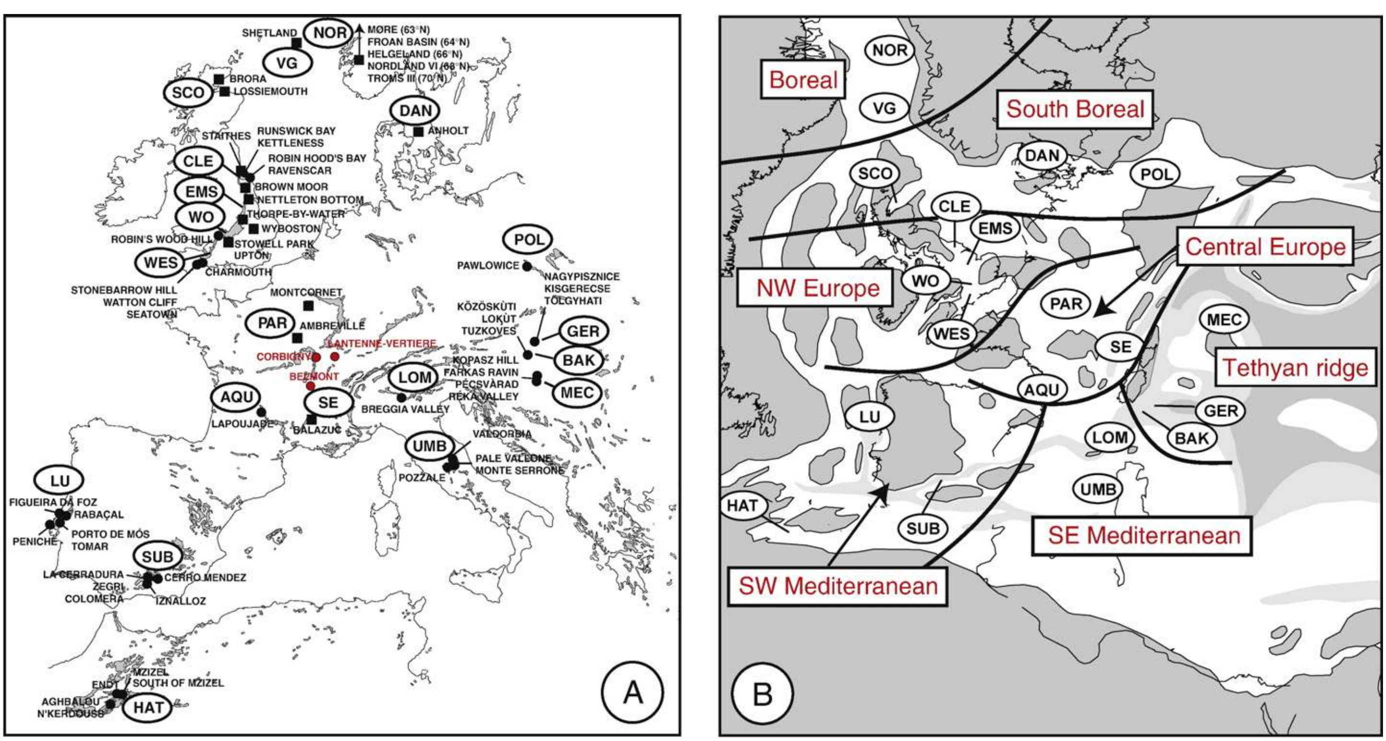

Fig. 2. (A) Locations of studied sections. Grey areas represent lower Jurassic outcrops, dark circles correspond to sections, and squares to boreholes. (B) Basins plotted on Toarcian palaeogeographic map (from Thierry et al., 2000b). NOR = Norwegian Sea; VG = Viking Graben; SCO = Scottish Basin; DAN = Danish Basin; POL = Polish Basin; CLE = Cleveland Basin; WO = Worcester Basin; EMS = East Midlands Shelf; WES = Wessex Basin; PAR = Paris Basin; SE = South East Basin; AQU = Aquitaine Basin; LU = Lusitanian Basin; SUB = Subbetic Basin; HAT = High Atlas Trough; LOM = Lombardian Basin; UMB = Umbria–Marche Basin; MEC = Mecsek Mountains; GER = Gerecse Mountains; BAK = Bakony Mountains.

Table 1
Information on lithology, palaeoenvironmental and diagenetic conditions for each studied section

Basin	Location	Clay mineralogy data references	Depositional environment	Main lithology	Burial depths and temperatures	T_{max} of organic matter (°C)
Aquitaine Basin	Lapoujade (France)	Brunel et al. (1999)	Deep marine	Mudstones	<2 km	430 to 438
Arabian Platform	Marrat (Saudi Arabia)	Abed (1979)	Infralittoral	Ferruginous sandstones	*Unknown*	<431
Bakony Mts	Tűzköves-árok (Hungary)	Viczián (1995)	Deep hemipelagic	Limestones	<3 km	425 to 440
Bakony Mts	Lókút (Hungary)	Viczián (1995)	Deep hemipelagic	Limestones	<3 km	425 to 440
Bakony Mts	Közöskúti-árok (Hungary)	Viczián (1995)	Deep hemipelagic	Limestones	<3 km	425 to 440
Cleveland Basin	Brown Moor (England)	Jeans (2006)	Intrashelf basin	Mudstones	4 km—100 to 120 °C	*Unknown*
Cleveland Basin	Staithes (England)	Jeans (2006), Kemp et al. (2005b)	Intrashelf basin	Mudstones and siltstones	4 km—100 to 120 °C	*Unknown*
Cleveland Basin	Ravenscar (England)	Kemp et al. (2005b)	Intrashelf basin	Laminated mudstones	4 km—100 to 120 °C	*Unknown*
Cleveland Basin	Robin Hood's Bay (England)	Kemp et al. (2005b)	Intrashelf basin	Laminated mudstones	4 km—100 to 120 °C	*Unknown*
Cleveland Basin	Kettleness (England)	Kemp et al. (2005b)	Intrashelf basin	Laminated mudstones	4 km—100 to 120 °C	*Unknown*
Cleveland Basin	Runswick Bay (England)	Kemp et al. (2005b)	Intrashelf basin	Laminated mudstones	4 km—100 to 120 °C	*Unknown*
Danish Basin	Anholt (Denmark)	Nielsen et al. (2003)	Proximal marine	Siltous shales	1.1 to 1.3 km	420 to 425
East Midlands Shelf	Nettleton bottom (England)	Jeans (2006)	Intrashelf basin	Mudstones and siltstones	3 km—75 to 90 °C	*Unknown*
East Midlands Shelf	Thorpe-by-water (England)	Jeans (2006)	Intrashelf basin	Mudstones and siltstones	3 km—75 to 90 °C	*Unknown*
East Midlands Shelf	Wyboston (England)	Jeans (2006)	Intrashelf basin	Mudstones and siltstones	3 km—75 to 90 °C	*Unknown*
Gerecse Mts	Nagypisznice (Hungary)	Viczián (1995)	Deep hemipelagic	Limestones	<3 km	425 to 440
Gerecse Mts	Kisgerecse (Hungary)	Viczián (1995)	Deep hemipelagic	Limestones	<3 km	425 to 440
Gerecse Mts	Tölgyháti (Hungary)	Viczián (1995)	Deep hemipelagic	Limestones	<3 km	425 to 440
Hida Marginal Terrane	Daira river area (Japan)	Goto and Tazaki (1998)	Proximal marine	Mudstones to sandy mudstones	*Unknown*	*Unknown*
High Atlas Rift	Aghbalou (Morocco)	Hadri (1993)	Shallow marine	Limestones/marls	<3 km	>500
High Atlas Rift	Endt (Morocco)	Brechbühler (1984)	Boundary of basin	Limestones/marls	4 to 5 km	>500
High Atlas Rift	South of Mzizel (Morocco)	Bernasconi (1983)	Deep basin	Limestones/marls (turbiditic)	8 km	>500
High Atlas Rift	Rich/Mzizel (Morocco)	Bernasconi (1983)	Deep basin	Limestones/marls (turbiditic)	8 km	>500
Lombardy Basin	Breggia Valley (Italy)	Deconinck and Bernoulli (1991)	Hemipelagic	Pelagic limestones and marls	*Unknown*	429 to 439
Lusitanian Basin	Peniche (Portugal)	Duarte (1998)	Outer submarine fan	Hemipelagic marls/turbidites	*Unknown*	420 to 450
Lusitanian Basin	Tomar (Portugal)	Duarte (1998)	Inner ramp	Bioclastic limestones	*Unknown*	400 to 445
Lusitanian Basin	Porto de Mós (Portugal)	Duarte (1998)	Outer ramp	Marly limestones	*Unknown*	400 to 445
Lusitanian Basin	Figueira da Foz (Portugal)	Duarte (1998)	Outer ramp	Marly limestones	*Unknown*	400 to 445
Lusitanian Basin	Rabaçal (Portugal)	Duarte (1998), Chamley et al. (1992)	Outer ramp	Marly limestones	*Unknown*	400 to 445
Mecsek Mts	Kopasz Hill (Hungary)	Raucsik and Merény (2000), Raucsik and Varga (2008)	Deep outer shelf	Mudstones and black shales	<3 km—130 to 150 °C	435
Mecsek Mts	Réka Valley (Hungary)	Raucsik and Merény (2000), Raucsik and Varga (2008)	Deep outer shelf	Black shales	<1 km—~100 °C	419 to 428
Mecsek Mts	Farkas Ravine (Hungary)	Raucsik and Merény (2000), Raucsik and Varga (2008)	Deep outer shelf	Mudstones	<1 km—50 to 100 °C	*Unknown*
Mecsek Mts	Pécsvárad (Hungary)	Raucsik and Merény (2000), Raucsik and Varga (2008)	Deep outer shelf	Mudstones	<3 km—130 °C	443
Norwegian Sea Basin	Troms III (Norway)	Mørk et al. (2003)	Shallow marine	Mudstones/locally silty	2.5 to 3 km	*Unknown*
Norwegian Sea Basin	Nordland VI (Norway)	Mørk et al. (2003)	Delta plain deposits	Mudstones	2.5 to 3 km	*Unknown*
Norwegian Sea Basin	Helgeland (Norway)	Mørk et al. (2003)	Shallow marine	Mudstones	2.5 to 3 km	*Unknown*
Norwegian Sea Basin	Froan Basin (Norway)	Mørk et al. (2003)	Shallow marine	Mudstones to sandstones	2.5 to 3 km	*Unknown*
Norwegian Sea Basin	Møre (Norway)	Mørk et al. (2003)	Proximal fan delta	Mudstones to sandstones	2.5 to 3 km	*Unknown*
Paris Basin	Montcornet (France)	Debrabant et al. (1992)	Offshore/shoreface	Mudstones (locally sandy)	<2 km	<430
Paris Basin	Ambreville (France)	Uriarte Goti (1997)	Basin	Mudstones	2.5 km	~435
Paris Basin	Corbigny (France)	This study	Basin	Mudstones	<2 km	<430
Paris Basin	Lantenne-Vertière (France)	This study	Deep marine	Mudstones	<2 km	<430
Polish Basin	Pawlowice (Poland)	Leonowicz (2005)	Proximal fan delta	Mudstones and silty mudstones	*Unknown*	*Unknown*
Scottish Basin	Brora (Scotland)	Hurst (1985a)	Proximal marine	Micaceous siltstones and shales	~2 km—50 to 60 °C	*Unknown*
Scottish Basin	Lossiemouth (Scotland)	Hurst (1985b)	Proximal marine	Siltstones	~2 km—>100 °C	*Unknown*
South East Basin	Belmont (France)	This study	Deep marine	Mudstones	>2 km	<443 ?
South East Basin	Balazuc (France)	Renac and Meunier (1995)	Marine	Limestones	>2 km—<130 °C	437
Subbetic Basin	Colomera (Spain)	Palomo-Delgado et al. (1985)	Deep marine	Limestones/marls	<1 km	*Unknown*
Subbetic Basin	Zegri (Spain)	Palomo-Delgado et al. (1985)	Shallow marine	Limestones/marls	<1 km	*Unknown*
Subbetic Basin	Cerro-Mendez (Spain)	Palomo-Delgado et al. (1985), Chamley et al. (1992)	Shallow marine	Limestones/marls	<1 km	*Unknown*
Subbetic Basin	La Cerradura (Spain)	Palomo-Delgado et al. (1985)	Shallow marine	Limestones/marls	<1 km	*Unknown*
Subbetic Basin	Iznalloz (Spain)	Chamley et al. (1992)	Shallow marine	Limestones/marls	<1 km	*Unknown*
Umbria–Marche	Pozzale (Italy)	Ortega-Huertas et al. (1993)	Hemipelagic	Mudstones	*Unknown*	424 to 435

(continued on next page)

Table 1 (*continued*)

Basin	Location	Clay mineralogy data references	Depositional environment	Main lithology	Burial depths and temperatures	T_{max} of organic matter (°C)
Basin						
Umbria–Marche Basin	Pale Vallone (Italy)	Ortega-Huertas et al. (1993)	Hemipelagic	Marls and Rosso Ammonitico	*Unknown*	424 to 435
Umbria–Marche Basin	Monte Serrone (Italy)	Ortega-Huertas et al. (1993)	Hemipelagic	Mudstones	*Unknown*	424 to 435
Umbria–Marche Basin	Valdorbia (Italy)	Ortega-Huertas et al. (1993), Monaco et al. (1994)	Hemipelagic	Mudstones (punctally detritic)	*Unknown*	424 to 435
Viking Graben	Well A 3/15 — 1&2 (Shetland)	Pearson (1990)	Proximal marine	Sandstones ?	>4.5 km	*Unknown*
Wessex Basin	Charmouth (England)	Jeans (2006)	Intrashelf basin	Mudstones	<2 km	420 to 430
Wessex Basin	Stonebarrow Hill (England)	Kemp et al. (2005b)	Intrashelf basin	Mudstones	<2 km	420 to 430
Wessex Basin	Watton Cliff (England)	Kemp et al. (2005b)	Intrashelf basin	Mudstones	<2 km	420 to 430
Wessex Basin	Seatown (England)	Kemp et al. (2005b)	Intrashelf basin	Mudstones	<2 km	420 to 430
Worcester Basin	Stowell Park (England)	Jeans (2006)	Intrashelf basin	Mudstones and siltstones	<3 km	*Unknown*
Worcester Basin	Upton (England)	Jeans (2006)	Intrashelf basin	Mudstones and siltstones	<3 km	*Unknown*
Worcester Basin	Robin's wood Hill (England)	Kemp et al. (2005b)	Intrashelf basin	Mudstones and siltstones	<3 km	*Unknown*

T_{max} data (temperature of maximum hydrocarbon generation during pyrolysis) are mainly from Baudin (1989), except for the Peniche section (Lusitanian Basin) where data are from Oliveira et al. (2006). Burial depth and temperature references are the same that clay mineralogy data references.

boreholes, whose mineralogical analyses were performed on bulk rocks (Mørk et al., 2003), only analyses carried out on the <2 µm fraction of sediments are included in the database. In addition, new data (available as Supplementary material) from the Paris Basin (Corbigny and Lantenne-Vertière quarries, France) and the South East Basin (Belmont quarry, France) were added to the database (Fig. 2A). Biostratigraphically located samples from these three outcrops, respectively dated Early Pliensbachian, Late Toarcian, and Toarcian, were analyzed using X-ray diffraction (Brucker D4 Diffractometer) on the <2 µm fraction, following the classical analytical procedure described by Moore and Reynolds (1997). As presented data are from various laboratories, we will bear in mind this possible bias when discussing the results. In addition, the impact of diagenetic and authigenic processes are evaluated or re-evaluated for each section to avoid misinterpretation in the significance of clay mineral assemblages. To this purpose, relevant information has been gathered from the literature (i.e., lithology, burial depth, T_{max} of organic matter), allowing these processes to be discriminated (Table 1).

Average raw clay mineral abundances from each locality have been calculated and plotted according to their biostratigraphic positions on palaeogeographic maps modified from Thierry et al. (2000a,b). Successive periods of focus are defined according to the ammonite biozonation of the NW Tethyan context. As far as possible, the degree of resolution reaches the biochronozone precision, but associations of consecutive zones were necessary, depending on the paucity of data or biostratigraphic uncertainties (e.g., the Late Toarcian). Eight time intervals were chosen (Fig. 3): 1) Jamesoni and Ibex Zones; 2) Davoei Zone; 3) Margaritatus Zone; 4) Spinatum Zone; 5) Tenuicostatum Zone; 6) Falciferum Zone; 7) Bifrons Zone; 8) Variabilis to Aalensis Zones. Data from southern Tethyan margins were correlated with data from the north using the Jurassic biostratigraphic synthesis proposed by Dommergues et al. (1997) and Elmi et al. (1997).

3. Results

3.1. Composition of clay assemblages

Clay mineral assemblages of the Peritethyan realm generally include five main clay minerals: chlorite, illite, kaolinite, smectite, and illite/smectite mixed-layers (I/S) (Fig. 4). Illite and kaolinite dominate the clay fraction, and their distribution seems mainly controlled by a latitudinal gradient. Kaolinite is dominant northwards, while illite proportions generally increase southwards. Smectite and I/S frequently occur but vary in proportion. Chlorite is often missing or is present in small proportions, except in the High Atlas (Morocco) where it is the dominant mineral (Bernasconi, 1983; Brechbühler, 1984; Hadri, 1993). Small amounts of vermiculite (<10%) are also occasionally present in sections from the eastern margin of the Paris Basin (Debrabant et al., 1992) and in the Lusitanian Basin (Chamley et al., 1992). Its absence in other sections may be related to frequent underestimations during diffractogram interpretations.

3.2. Variations of kaolinite content over time

In order to test the palaeoclimatic significance of Early Jurassic clay minerals, we focus on kaolinite because its abundance in modern sediments expresses a strong climatic dependence monitored by chemical weathering intensity (Chamley, 1989). The resistance of kaolinite to moderate diagenetic influences is another advantage of this mineral by comparison with smectite or I/S, which are more easily transformed into illite during incipient diagenetic processes (Thiry, 2000). Fig. 5 illustrates spatiotemporal fluctuations of kaolinite amounts between successive periods. Only changes of 5% or more are considered significant and reliable.

Four key periods of kaolinite variations are discussed: (1) From the Jamesoni to Davoei Zones, kaolinite proportions generally increase in sediments from northern areas (southern data are unfortunately lacking for this transition). (2) This rise is followed by an interval, encompassing the Davoei to Tenuicostatum Zones, during which proportions stay almost constant or gradually decrease for most Peritethyan areas. Some basins such as the Bakony or East Midlands Shelf basins still record occasional kaolinite enrichments. (3) The transition between the Tenuicostatum and Falciferum Zones marks the beginning of a reversed trend, with significant increases of kaolinite, although some locations still present invariant proportions. This trend is also observed during the Bifrons Zone, except in some sections from the Lusitanian and Subbetic basins where the kaolinite proportion slightly decreases (Chamley et al., 1992; Duarte, 1998). (4) Finally, kaolinite content depletes everywhere during the Late Toarcian.

3.3. Spatial distribution of clay minerals

Average proportions of clay minerals were calculated according to spatial contexts for the whole of the studied period (Fig. 6). Detailed analyses of clay mineral distribution at each interval were avoided because of the unequal quality and quantity of data over time and space. Basins were grouped into the following domains, independently of palaeobiogeographic provinces (Fig. 2B): Boreal Europe (NOR

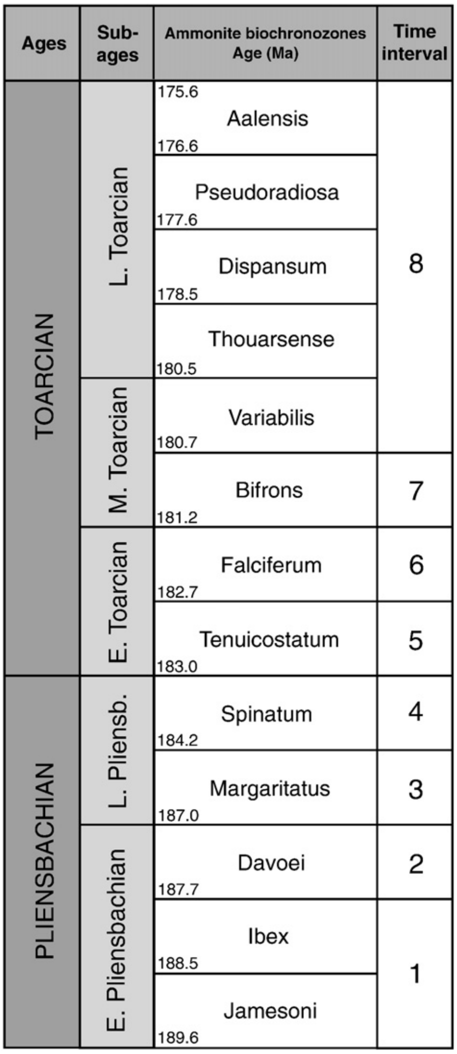

Fig. 3. NW Tethyan biostratigraphic time scale (Pliensbachian and Toarcian). Isotopic ages are from Gradstein et al. (2004).

and VG), South boreal Europe (SCO, DAN, POL), North West Europe (CLE, EMS, WO, WES), Central Europe (PAR, AQU, SE), Tethyan oceanic ridge (MEC, BAK, GER), South West Mediterranean (LU and SUB), South East Mediterranean (LOM and UMB). Data from Saudi Arabia and Japan were also included (Abed, 1979; Goto and Tazaki, 1998), but those from the High Atlas of Morocco were not considered because of excessive burial diagenesis (see Section 4.1).

We notice a clear difference in clay mineral distribution between the northern and southern Peritethyan margins over the Pliensbachian–Toarcian interval (Fig. 6). In boreal zones, kaolinite is dominant (~50%) and illite proportions are low (25%). Between 40 ° N and 30 ° N, kaolinite amounts are lower (~38% in South Boreal Europe to ~28% in NW Europe) while those of illite are higher (between 32% and 19%). At equivalent latitudes, sediments from Japan show comparable proportions of kaolinite but higher amounts of illite (~50%). At lower latitudes (25° N to 20° N), there is a surge of illite (between 65% and 75%), offset by a significant depletion of kaolinite (~10%). The trend is reversed around the palaeoequator, where kaolinite becomes dominant (~75%) by comparison with illite (20%).

The dispersal of smectite and I/S seems less dependent on latitude. Proportions, comprised between 15 and 30%, are slightly reduced towards the southern Tethyan margins, and become close to 0% in Japan and around the palaeoequator. Chlorite, while widespread, never exceeds 12% of the clay fraction. This clay species is absent in the SE Mediterranean and around the palaeoequator.

4. Discussion

4.1. Diagenetic and authigenic influences

After deposition, clay mineral assemblages suffer diagenetic changes because of fluid circulation through porosity and dehydration during compaction. During early diagenesis, meteoritic water circulation may remove alkali elements in solution, leading to the development of authigenic kaolinite. The occurrence of authigenic kaolinite is often evidenced by clear relationships between lithology and clay mineralogy. Sandstones, being highly porous, are often enriched in authigenic kaolinite by comparison with adjacent argillaceous sediments. Other processes such as halmyrolytic alterations of basement basalts or volcanic ashes may also produce neoformed clay minerals, particularly in the context of hydrothermal activity. In modern deep ocean basins, authigenic smectite is considered the predominant clay mineral (Clauer et al., 1990). Burial diagenesis is also responsible for the progressive illitization of original smectite. In sedimentary successions, massive illitization of smectite is evidenced by the progressive decrease of smectite offset by increasing I/S and illite with depth (Lanson and Meunier, 1995). Thus, before any palaeoenvironmental interpretation of clay mineral assemblages, it is necessary to estimate the overprint of these processes for each basin. Burial depth and T_{max} values are usually suitable indices of diagenetic intensity, assuming that significant illitization of smectite starts when burial depth reaches about 2000 m and/or when T_{max} reaches 430/440 °C (Burtner and Warner, 1986; Chamley, 1989).

Precipitation of vermicular kaolinite related to dissolution of K-feldspar has been demonstrated in sections from the Norwegian Sea Basin (Mørk et al., 2003), implying an overestimation of kaolinite. Moreover, the alternative analytical method (i.e., bulk analysis) probably enhances the proportion of this clay species. Owing to significant burial depths (between 2.5 and 3 km), illitization processes are also very common in this area (Pearson, 1990). In South Boreal domains, authigenic kaolinite has been reported in siltstones from the Scottish Basin only (Hurst, 1985a,b). Except for the Danish Basin, where low burial depths (~1.5 km) and low T_{max} (~420 °C on average) suggest a lack of diagenetic overprint (Nielsen et al., 2003), smectite from South Boreal areas has been transformed into I/S, implying incipient illitization in spite of low burial depths.

In the NW European domain, Pliensbachian–Toarcian strata were buried at different depths. These were less than 2 km in the Wessex Basin but gradually reached 4 km in the Cleveland Basin (Kemp et al., 2005b). Moderate T_{max} values (420 to 430 °C) have been reported from southern basins, and consequently, smectite is still preserved. In northern basins, smectite has been transformed into I/S or illite. Following Kemp et al. (2005b), we think that the difference of diagenetic context may have triggered gradual northwards illitization and chloritization of sediments. In addition, during a period of generalized kaolinite depletion at the Margaritatus–Spinatum Zone transition, sediments from the East Midlands Shelf record an abnormal kaolinite enrichment (Fig. 5), probably related to sporadic diagenetic berthierine concentrations (iron-rich kaolinite variety) (Jeans, 2006).

In central European domains, diagenetic overprints are contrasted. On the Paris Basin borders, the ~2 km burial depth and the ~430 °C T_{max} values suggest incipient to moderate illitization and chloritization (Delavenna et al., 1989; Debrabant et al., 1992). In its central part, Uriarte Goti (1997) suggests that sediments reach the oil window (~2.5 km burial depth). Consequently, diagenetic processes could have been more significant. Chloritization and illitization of smectite cannot be excluded in the Aquitaine and South East basins of France owing to T_{max} respectively reaching ~435 and ~440 °C.

Because of their proximity to the Western Tethyan oceanic ridge, clay minerals from the Bakony and Gerecse Mountains might have been sporadically affected by hydrothermal weathering (Viczián,

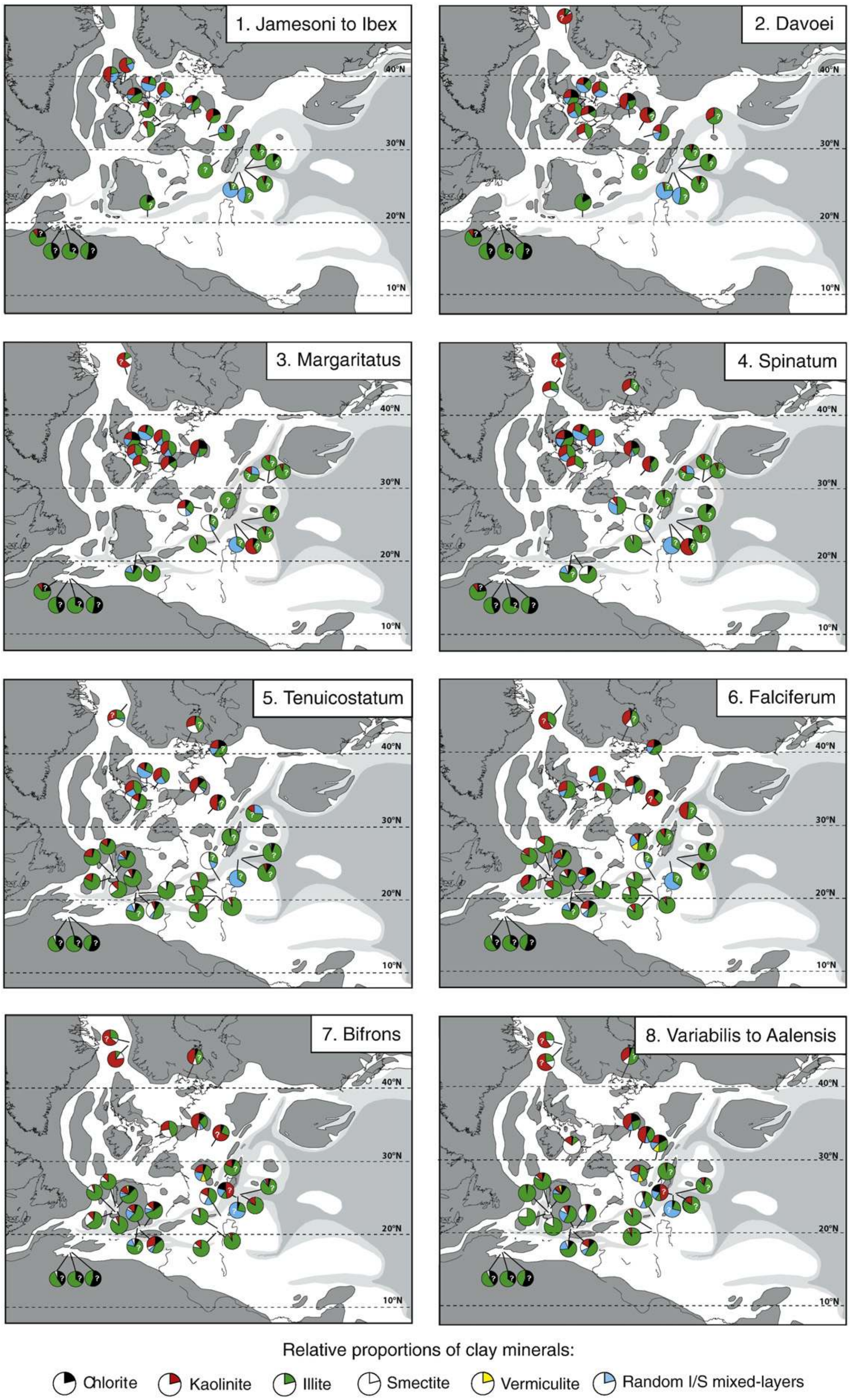
1. Jamesoni to Ibex
2. Davoei
3. Margaritatus
4. Spinatum
5. Tenuicostatum
6. Falciferum
7. Bifrons
8. Variabilis to Aalensis
40°N
30°N
20°N
10°N
Relative proportions of clay minerals:
Chlorite
Kaolinite
Illite
Smectite
Vermiculite
Random I/S mixed-layers

1995). This is illustrated during the Davoei–Margaritatus Zone transition by abnormal (about 60%) kaolinite enrichments in the Bakony area (Fig. 4). We suppose that this anomaly corresponds to local hydrothermal dickite/nacrite neoformations. Mudstones from the Bakony and Gerecse Mountains were buried at depths estimated between 2 and 3 km and indicate T_{max} between 425 and 440 °C. Therefore, we think that sediments from these areas have been partly illitized. For the Mecsek Mountains, Raucsik and Varga (2008) suggest an absence of diagenetic influences owing to low burial depths (~1 km).

In the Eastern Mediterranean domains, smectite is often preserved and/or transformed into I/S. T_{max} varies between 429 and 439 °C in the Lombardian Basin, and some diagenetic transformations are supposed (Deconinck and Bernoulli, 1991). In the Umbria–Marche Basin, T_{max} fluctuates between 424 and 435 °C, implying more moderate illitization processes. This would mean that a significant part of the huge illite amounts observed are detrital in origin (Ortega-Huertas et al., 1993).

In the Western Mediterranean domains, diagenetic overprints are more contrasted. The burial depth of Pliensbachian–Toarcian sediments is estimated at ~1 km in the Subbetic Basin, and illitization processes are assumed to have been very rare (Palomo-Delgado et al., 1985; Chamley et al., 1992). In the Lusitanian Basin, T_{max} generally varies between 400 and 450 °C (Baudin, 1989; Oliveira et al., 2006), revealing probably more pronounced illitization. Sediments from the High Atlas are completely illitized and chloritized owing to deep burial (3 to 8 km) and are thus not interpretable in terms of palaeoenvironments (Bernasconi, 1983; Brechbühler, 1984; Hadri, 1993).

Outside the Peritethyan realm, authigenic kaolinite is reported in sandstones from Saudi Arabian sections (Abed, 1979). T_{max} values are moderate (<431 °C) and suggest limited illitization. In the Japanese domain, some of the kaolinite is probably authigenic too owing to the porosity of sediments, and the smectite may have been illitized or chloritized because of the high geothermal gradient of the subduction zone.

To summarize, illitization of smectite is prevalent in Peritethyan sections. This process relies heavily on the local tectonic, burial, and thermal evolution of each area, which can be markedly different from one section to another (Fig. 6; Table 1). Estimating diagenetic transformations and proportions of neoformed clay minerals remains difficult then. Only sediments from Boreal and South Boreal areas are affected by kaolinite authigenesis because they tend to be more siliciclastic, coarse and porous. In the other Peritethyan sections, kaolinite is interpreted as mainly detrital, and may reflect palaeoenvironmental conditions. Therefore, to strengthen the interpretation of latitudinal and temporal variations of clay minerals, we focus on sediment kaolinite content alone.

4.2. Reliability of kaolinite as a palaeoenvironmental proxy

Despite the occurrence of diagenetic transformations in some sections, several arguments point to the preservation of a primary palaeoenvironmental signal in the evolution of kaolinite content through the Pliensbachian–Toarcian interval:

1) As geodynamic evolution and sedimentation are specific to each basin, common diagenetic processes cannot be responsible for simultaneous rises of kaolinite throughout the Peritethyan Realm.
2) Most sections exhibit reversible vertical trends in kaolinite content, and there is no evidence of progressive change with depth. This suggests that burial diagenesis was never strong enough to transform the initial kaolinite into illite and/or chlorite. The classic scheme of kaolinite diagenesis generally proposes progressive transformations into dickite or nacrite near metamorphic contexts, but unlike smectite, kaolinite displays greater resistance to illitization under moderate diagenetic conditions (Lanson et al., 2002). Here, the only exception concerns sediments from the High Atlas of Morocco, where kaolinite is invariably absent.
3) Except for abnormal kaolinite enrichments recorded in the Bakony area and in the East Midlands Shelf during the Late Pliensbachian (see above) (Fig. 5), we exclude any differential diagenetic process concerning other Peritethyan sections because outcrops never present important variations of lithology and porosity through time. Even if some sections have been affected by authigenic processes—illitization or chloritization—we think that enrichments in neoformed kaolinite or impoverishments linked to diagenetic transformations have been homogenous through sediment thickness. Consequently, absolute proportions of kaolinite may be slightly enhanced or diminished, but the initial signal of kaolinite variations should not be too greatly disturbed.

Through each interval, kaolinite contents fluctuate in the same way, independently of the palaeogeographic context. We suggest that variations are dictated by broad-scale palaeoenvironmental factors. Some local causes may however interact and disturb the regional trend (Fig. 5). The most illustrative example occurs at the transition between the Falciferum and Bifrons Zones, during which relative proportions of kaolinite slightly and locally decrease in some sections from the SW Mediterranean area, while they increase everywhere else in the Peritethyan Realm. This contrary behaviour in the SW Mediterranean area could be tentatively explained by local modifications of the source of clay minerals.

4.3. Palaeoclimatic variations

Thermal variations of Pliensbachian and Toarcian seawater have been widely studied using the oxygen isotope compositions of belemnite guards. As belemnite $\delta^{18}O$ values and belemnite Mg/Ca data (a temperature proxy independent of $\delta^{18}O_{seawater}$ fluctuations) exhibit similar variations, it has been suggested that belemnite $\delta^{18}O$ is reliable for estimating seawater temperatures for this period (Rosales et al., 2004). Several warming and cooling phases have been identified (Fig. 7): the Pliensbachian is characterized by a warming event during its first part, with a thermal maximum during the Davoei Zone, followed by a significant cooling during the Late Pliensbachian, with the coldest temperatures recorded during the Spinatum Zone. This period is followed by a warming from the Pliensbachian–Toarcian boundary to the Bifrons Zone, with a drastic temperature rise coeval with the Early Toarcian OAE. Seawater temperatures decrease during the Thouarsense Zone, and remain rather stable during the Late Toarcian. Short-term warming events were also reported between the Dispansum and Pseudoradiosa Zones, but additional data are needed to confirm these results (Gómez et al., 2008).

Alongside $\delta^{18}O$, $\delta^{13}C$, and Mg/Ca excursions marking the Early Toarcian OAE (Falciferum Zone), Cohen et al. (2004) highlight important shifts of weathering proxies such as seawater strontium or osmium isotopes, and interpret this as indicative of a transient acceleration of chemical weathering rates (estimated between 400% and 800%), resulting from warmer temperatures and enhanced rainfall. Two additional slope breaks can be identified on the $^{87}Sr/^{86}Sr$ curve during the Davoei and Bifrons Zones when data are plotted against absolute ages (Jones et al., 1994) (Fig. 7). Following Cohen et al. (2004), we argue here that brief accelerated rises of $^{87}Sr/^{86}Sr$ during the Falciferum and Bifrons Zones within a long term $^{87}Sr/^{86}Sr$ increase may similarly reflect enhanced weathering rates. In the same

Fig. 4. Distribution of clay minerals in palaeogeographic contexts according to the eight time intervals. Maps are from Thierry et al. (2000a,b) and correspond to the Sinemurian map for the two first sketches, and to the Toarcian map for the others. Question marks indicate biostratigraphic uncertainties.

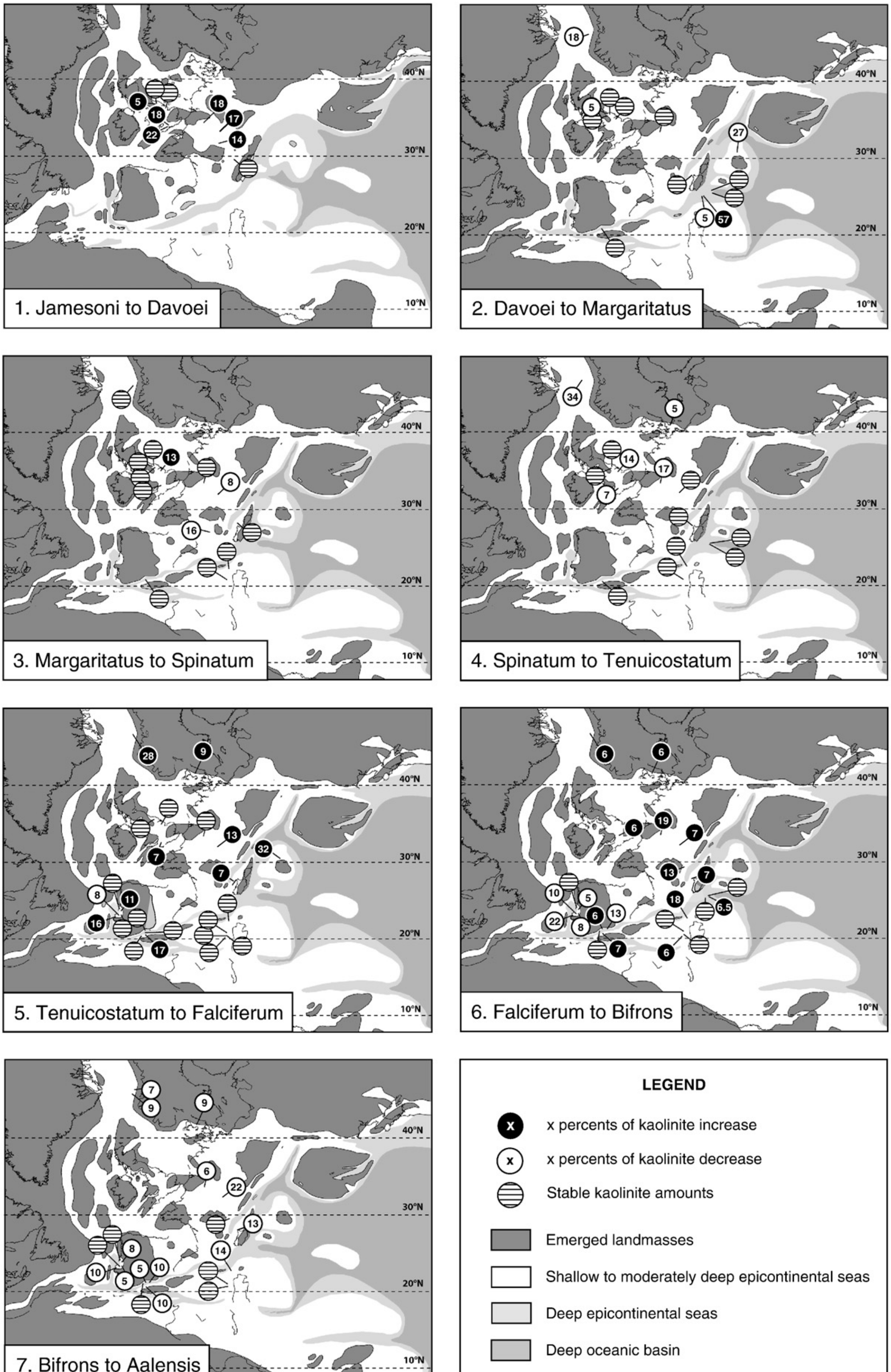

Fig. 5. Variations of kaolinite abundance over the Pliensbachian/Toarcian period. Each map represents the transition between two successive time intervals.

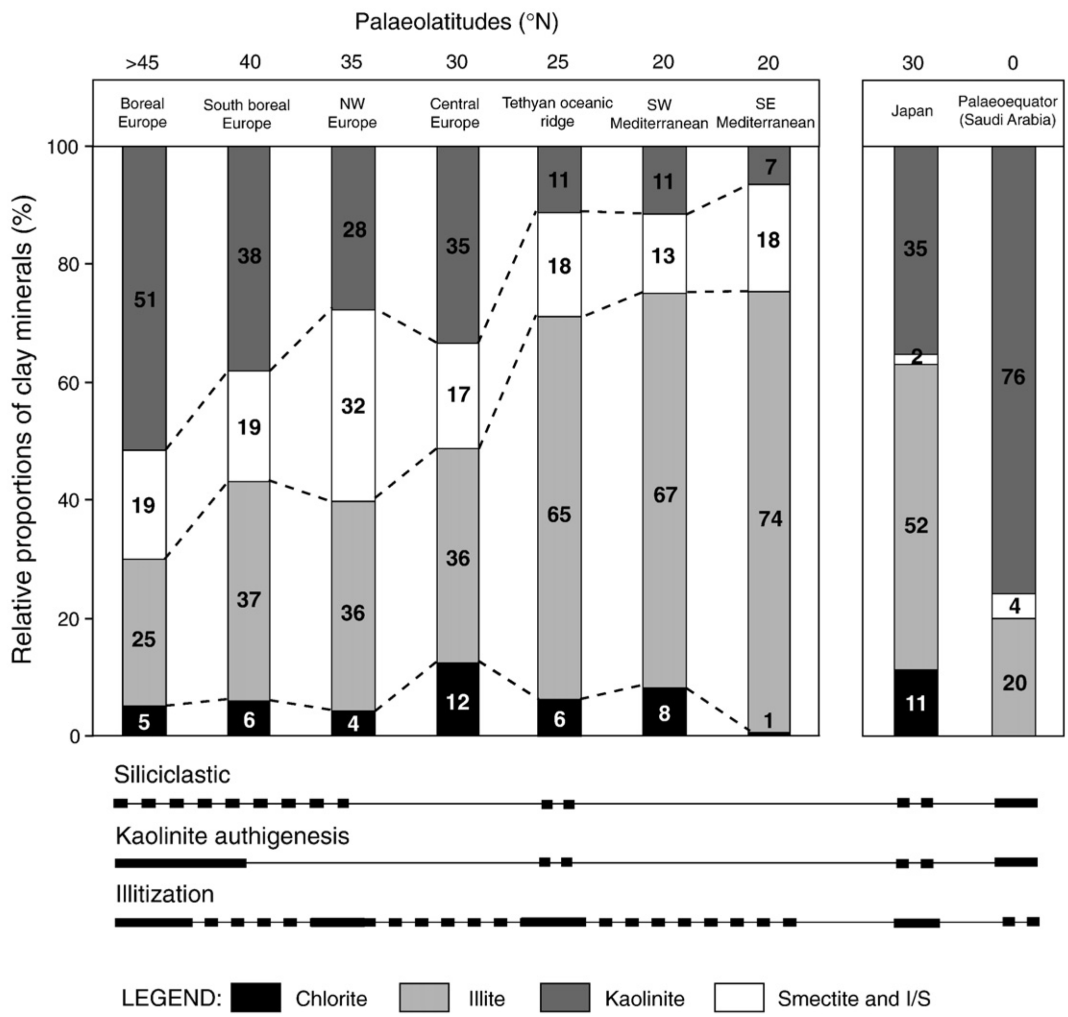

Fig. 6. Average proportions of clay minerals according to palaeolatitudinal contexts over the Pliensbachian–Toarcian period. Presence of siliciclastic materials, kaolinitic authigenesis, and illitizations are also indicated.

way, the plateau on the $^{87}Sr/^{86}Sr$ curve characterizing the Davoei Zone may be related to enhanced continental weathering during a period of generalized $^{87}Sr/^{86}Sr$ fall, characterizing an interval of hydrothermal activity (Jones and Jenkyns, 2001). Interestingly, these three $^{87}Sr/^{86}Sr$ slope breaks are consistent with variations of temperature proxies, implying that warm periods were wet and that cooler periods were more arid during the Pliensbachian–Toarcian interval.

The evolution of kaolinite content in sediments corresponds to these short-term (~1 My) climate variations (Fig. 7). During periods of warming and rises of $^{87}Sr/^{86}Sr$, kaolinite abundance increases. Thus, kaolinite enrichments in sediments during the Davoei Zone and during the Early and Middle Toarcian reinforce, in conjunction with strontium isotope fluctuations, the scheme of enhanced landmass weathering during these intervals. Conversely, cooler and drier intervals have led to low hydrolyses and weak leaching of the substratum, implying a decrease of kaolinite counterbalanced by smectite and/or illite enrichments. These broad-scale results therefore confirm the strong influence of palaeoclimatic changes on kaolinite enrichments in sediments, as has been discussed in previous studies (e.g., Hallam et al., 1991; Diekmann et al., 1996; Deconinck et al., 2003; Ahlberg et al., 2003; Pellenard and Deconinck, 2006; Schnyder et al., 2006; Raucsik and Varga, 2008).

The absence of delay between the establishment of warm/wet climate and the beginning of kaolinite enrichments in sediments may appear surprising. According to Thiry (2000), 1 to 2 My generally elapse between the time of clay formation in soils and their occurrence in marine sediments owing to the slow formation rate of soils and the timing of erosional processes which may occur a long time after. However, as data point to synchronism between kaolinite enrichments and palaeoclimatic variations, we suggest that the formation of kaolinite on continents and its deposition in marine sediments could be almost contemporaneous during the Early Jurassic (less than 100 ky).

4.4. Kaolinite distribution and sources

In modern oceans, abundant kaolinite near tropical regions expresses a strong climatic dependence dictated by the zonation of chemical weathering intensity (Chamley, 1989). The palaeolatitudinal distribution of kaolinite contents in sediments during the Pliensbachian–Toarcian could therefore reflect palaeoclimatic belts with contrasted hydrolyzing conditions. From 45° N to 30° N, the abundance of kaolinite in Peritethyan domains suggests wet conditions, allowing the development of thick, well-drained, acid soils characteristic of subtropical zones. Sediments from Japan located at the same latitudes exhibit similar proportions, supporting the idea of an extensive wet belt. Conversely, kaolinite becomes rare from 25° N to 20° N, suggesting a drier climatic belt. Partial data from the Toarcian of Tunisia show similar values (Jamoussi et al., 2003), indicating that

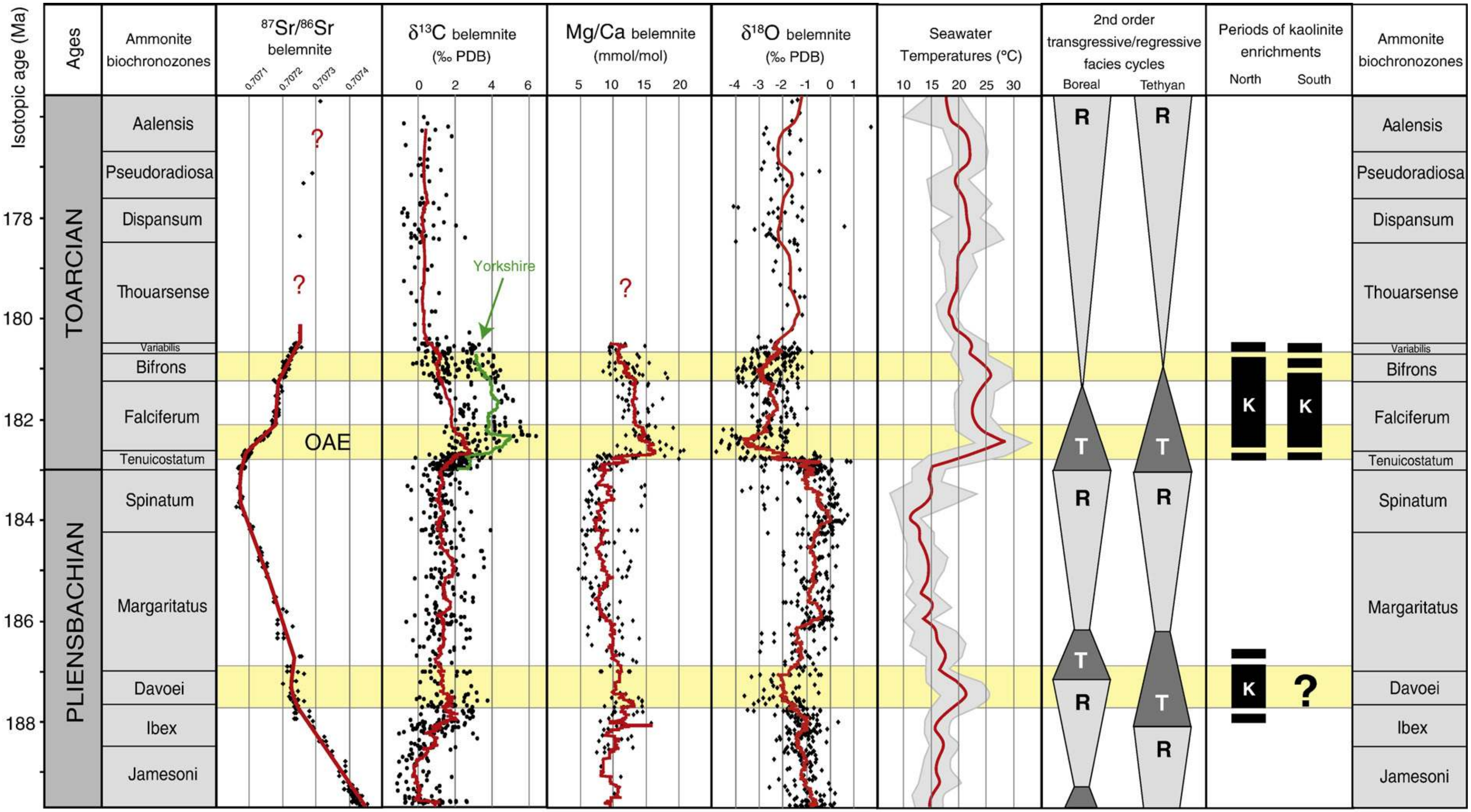

Geochemical data references:

$^{87}Sr/^{86}Sr$ data : Jones et al. (1994), Hesselbo et al. (2000b), McArthur et al. (2000), and Jenkyns et al. (2002)
Mg/Ca data : McArthur et al. (2000), Bailey et al. (2003), Rosales et al. (2004), and Van de Schootbrugge et al. (2005b)
$\delta^{13}C$ and $\delta^{18}O$ data : Hesselbo et al. (2000b), McArthur et al. (2000), Jenkyns et al. (2002), Bailey et al. (2003), Rosales et al. (2004), Metodiev and Koleva-Rekalova (2006), Van de Schootbrugge et al. (2005b), and Gómez et al. (2008)

Fig. 7. Comparison between geochemical palaeoenvironmental proxies and kaolinite enrichments in sediments. Belemnite $\delta^{18}O$, $\delta^{13}C$, $^{87}Sr/^{86}Sr$, and Mg/Ca data from several localities (i.e., UK, Germany, Portugal, Spain, and Bulgaria) are compiled from literature, and used to build new composite geochemical curves. $\delta^{18}O$ values have been translated into temperatures using the equation of Anderson and Arthur (1983) and assuming a $\delta^{18}O_{seawater}$ of −1‰ (no ice cap). Temperature variations are represented by a running mean curve and standard deviations. Yellow bands indicate periods where $\delta^{18}O$, $\delta^{13}C$, and Mg/Ca excursions are concomitant with $^{87}Sr/^{86}Sr$ slope breaks. Second order transgressive/regressive cycles are from Hardenbol et al. (1998). Geochemical data references: **$^{87}Sr/^{86}Sr$ data:** Jones et al. (1994), Hesselbo et al. (2000b), McArthur et al. (2000), and Jenkyns et al. (2002). **Mg/Ca data:** McArthur et al. (2000), Bailey et al. (2003), Rosales et al. (2004), and Van de Schootbrugge et al. (2005b). **$\delta^{13}C$ and $\delta^{18}O$ data:** Hesselbo et al. (2000b), McArthur et al. (2000), Jenkyns et al. (2002),Bailey et al. (2003), Rosales et al. (2004), Metodiev and Koleka-Rekalova (2006), Van de Schootbrugge et al. (2005b), and Gómez et al. (2008).

the semiarid belt would reach zones located at 15° N. Finally, around the palaeoequator, even if some of the kaolinite is of authigenic origin, the proportion of detrital kaolinite seems significant, indicating a tropical climate favouring the development of kaolinite-rich lateritic soils (Abed, 1979). This climatic inference about the distribution of kaolinite is consistent with reconstructions using palaeophytogeographic, sedimentary data, and GCM modelling approaches. Chandler et al. (1992) and Rees et al. (2000) differentiate temperate climates characterized by megamonsoons beyond 30° N, a semiarid belt from 30° N to 15° N, and a summerwet climate at the palaeoequator (Fig. 8). Palaeobiogeographic data based on ammonites or bivalves also indicate a differentiation of Euro-boreal and Tethyan provinces, which may reflect a palaeoenvironmental or palaeoclimatic boundary (Enay and Mangold, 1982; Mouterde and Elmi, 1991; Liu et al., 1998). This congruence between independent approaches supports the identification of palaeoclimatic belts and, moreover, humidity and temperature as the major controls on the distribution of kaolinite during the Pliensbachian–Toarcian interval.

Hurst (1985a,b) argues that enhanced humidity during the Early Jurassic was insufficient to generate such an abundance of kaolinite in northern Peritethyan domains, suggesting alternative sources of detrital kaolinite to soils. The hypothesis of a reworking of kaolinite-bearing sedimentary rocks formed during the Hercynian cycle was therefore proposed. Devonian and Carboniferous sedimentary series are generally considered as potential sources, because of their high proportions of detrital and/or authigenic kaolinite (Shaw, 2006; Spears, 2006; Hillier et al., 2006). From the Late Triassic to Early Jurassic, these Palaeozoic regoliths, which were highly developed in northern areas, would have been uplifted and weathered, so acting as a significant source of kaolinite.

In parallel, differential settling of kaolinite versus smectite related to basin structuring has probably enhanced the latitudinal segregation of clay minerals. Because of their large size, kaolinite particles are generally deposited near the shoreline, whereas smectite particles, being smaller, are deposited further from the source (Gibbs, 1977). As northern Peritethyan basins were mostly characterized by shallow to moderately deep marine environments surrounded by continents and punctuated by numerous archipelagos, proximal kaolinite inputs were favoured. Conversely, southern Peritethyan environments more distant from large continental sources may imply a depletion of kaolinite deposits, especially in the SE Mediterranean and around the Tethyan Ridge.

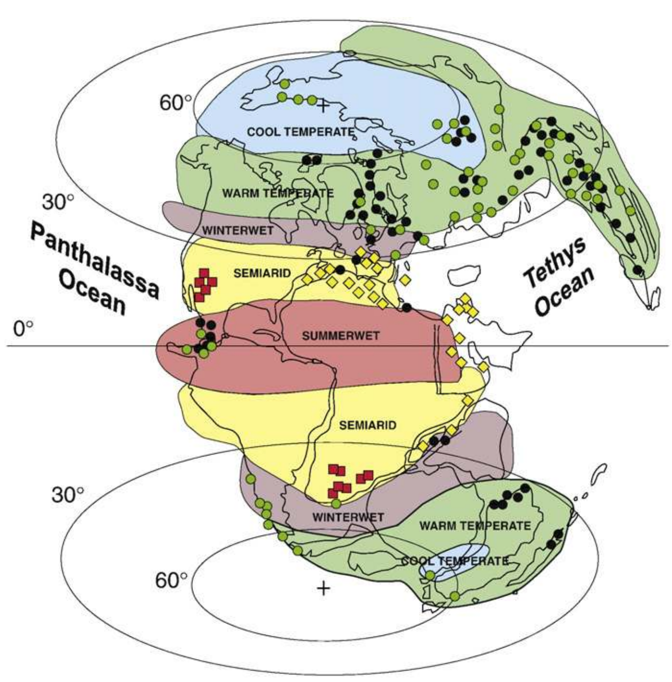

Fig. 8. Early Jurassic palaeoclimatic belts inferred from sedimentological and palaeophytogeographic data from Rees et al. (2000) and Arias (2007).

The impact of each factor is still hard to determine and it is likely that they act in conjunction or alternately. Nevertheless, the formation of subtropical kaolinitic soils and/or the reworking of Hercynian kaolinitic substrata involve strong runoffs on northern landmasses, suggesting that northwards kaolinite enrichments reflect a humid climate and a subsequent deposition of sediments in proximal basins. Clarifying relationships between the distribution of clay minerals and warming/cooling events remains of prime importance to highlight latitudinal climatic factors, but this requires a multiplication of biostratigraphically-constrained clay mineral data both in northern and southern domains.

5. Conclusions

After a broad-scale analysis of variations and distribution of clay minerals during the Pliensbachian–Toarcian interval, different points may be highlighted:

1) Once diagenetic overprints have been identified and eliminated for each section, clay minerals (especially kaolinite) can be considered as reliable palaeoclimatic proxies for the Pliensbachian–Toarcian interval. Major kaolinite enrichments occur in parallel to short-term strontium isotope fluctuations during the Davoei, Falciferum and Bifrons Zones, suggesting a humid climate with enhanced runoff during warm periods evidenced by $\delta^{18}O$ and Mg/Ca data. Conversely, cooler and drier intervals such as the Late Pliensbachian or the Late Toarcian imply low hydrolysis of landmasses, leading to the depletion or stabilization of kaolinite contents. In addition, we observe that the delay between the formation of kaolinite and its deposition in marine sediments was very short.
2) Secondary factors may sporadically disturb the palaeoclimatic signal. Local events such as the early interruption of kaolinite enrichments in the SW Mediterranean could be related to modifications of sources. Abnormal and local surges of kaolinite may also be linked to particular diagenetic or hydrothermal events. This enhances the need for a broad-scale (at least regional) approach to clearly identify major palaeoclimate changes.
3) This study highlights a latitudinal dispersal of kaolinite, with significant enrichments towards northern parts of the Peritethyan realm. This pattern is clearly enhanced by kaolinite neoformations in Boreal and South Boreal areas, but even if these data are discriminated, the latitudinal segregation remains apparent, implying a probable control by environmental parameters. Northwards kaolinite enrichments may be explained by: 1) a humid climate towards high palaeolatitudes favouring the development of kaolinite-rich soils; 2) a weathering of a pre-Jurassic kaolinitic substratum on northern landmasses; 3) a proximal sedimentation controlled by basin structuring.

Acknowledgements

This paper is a contribution by the SEDS “Système, Environnements, et Dynamique Sédimentaire” and FED “Forme, Évolution, Diversité” teams of the CNRS Biogéosciences laboratory. We thank F. Surlyk, S.P. Hesselbo and an anonymous reviewer for their constructive comments which improved the manuscript.

Appendix A. Supplementary data

Supplementary data associated with this article can be found, in the online version, at doi:10.1016/j.palaeo.2008.09.010.

References

Abed, A.M., 1979. Lower Jurassic lateritic redbeds from central Arabia. Sediment. Geol. 24, 149–156.

Ahlberg, A., Olsson, I., Šimkevičius, P., 2003. Triassic–Jurassic weathering and clay mineral dispersal in basement areas and sedimentary basins of southern Sweden. Sediment. Geol. 161, 15–29.

Anderson, T.F., Arthur, M.A., 1983. Stable isotopes of oxygen and carbon and their application to sedimentologic and paleoenvironmental problems. In: Arthur, M.A., Anderson, T.F., Kaplan, I.R., Veizer, J., Land, L.S. (Eds.), Stable Isotopes in Sedimentary Geology. SEPM Short Course, vol. 10, pp. 1–151. Tulsa.

Arias, C., 2007. Pliensbachian–Toarcian ostracod biogeography in NW Europe: Evidence for water mass structure evolution. Palaeogeogr. Palaeoclimatol. Palaeoecol. 251, 398–421.

Bailey, T.R., Rosenthal, Y., McArthur, J.M., Van de Schootbrugge, B., Thirwall, M.F., 2003. Paleoceanographic changes of the Late Pliensbachian–Early Toarcian interval: a possible link to the genesis of an Oceanic Anoxic Event. Earth Planet. Sci. Lett. 212, 307–320.

Baudin, F., 1989. Caractérisation géochimique et sédimentologique de la matière organique du Toarcien Téthysien (Méditerranée, Moyen-Orient), significations paleogéographiques. Ph.D. Thesis, Univ. Paris 6, Paris, France.

Bernasconi, R., 1983. Géologie du Haut-Atlas de Rich (Maroc). Ph.D. Thesis, Univ. of Neuchâtel, Neuchâtel, Switzerland.

Biscaye, B.E., 1965. Mineralogy and sedimentation of recent deep sea clay in the Atlantic Ocean and adjacent seas and oceans. Geol. Soc. Am. Bull. 76, 803–832.

Bout-Roumazeilles, V., Combourieu Nebout, N., Peyron, O., Cortijo, E., Landais, A., Masson-Delmotte, A., 2007. Connection between South Mediterranean climate and North African atmospheric circulation during the last 50,000 yr BP North Atlantic cold events. Quaternary Sci. Rev. 26, 25–28.

Brechbühler, Y.A., 1984. Étude structurale et géologique du Haut Atlas calcaire entre le Jebel Ayachi et Rich (Maroc), Ph.D. Thesis, Univ. of Neuchâtel, Neuchâtel, Switzerland.

Brunel, F., Rey, J., Cubaynes, R., Deconinck, J.-F., Emmanuel, L., Lachkar, G., 1999. Caractérisation sédimentologique, minéralogique, géochimique et palynologique des cortèges sédimentaires du Domérien du Quercy septentrional (Nord-Est du Bassin d'Aquitaine). Bull. Soc. Géol. France 170, 475–486.

Burtner, R.L., Warner, M.A., 1986. Relationship between illite/smectite diagenesis and hydrocarbon generation in Lower Cretaceous Mowry and Skull Creek Shales of the northern Rocky Mountain area. Clays and Clay Minerals 34, 390–402.

Cecca, F., Macchioni, F., 2004. The two Early Toarcian (Early Jurassic) extinction events in ammonoids. Lethaia 37, 35–56.

Chamley, H., 1989. Clay Sedimentology. Springer Verlag, Berlin.

Chamley, H., Baudin, F., Fourcade, E., Galbrun, B., 1992. Stratigraphie minéralogique des argiles du Toarcien d'Ibérie méridionale et occidentale. Ann. Soc. Géol. Nord 2, 109–117.

Chandler, M.A., Rind, D., Ruedy, R., 1992. Pangean climate during the Early Jurassic: GCM simulations and the sedimentary record of paleoclimate. Geol. Soc. Am. Bull. 104, 543–559.

Clauer, N., O'Neil, J.R., Bonnot-Courtois, C., Holtzapffel, T., 1990. Morphological, chemical, and isotopic evidence for an early diagenetic evolution of detrital smectite in marine sediments. Clays Clay Miner. 38, 33–46.

Cohen, A.S., Coe, A.L., Harding, S.M., Schwark, L., 2004. Osmium isotope evidence for the regulation of atmospheric CO_2 by continental weathering. Geology 32, 157–160.

Damborenea, S.E., 2002. Jurassic evolution of Southern Hemisphere marine palaeobiogeographic units based on benthonic bivalves. Geobios 35, Mém. Spec. 24, 51–71.

Debrabant, P., Chamley, H., Deconinck, J.-F., Récourt, P., Trouiller, A., 1992. Clay sedimentology, mineralogy and chemistry of Mesozoic sediments drilled in the Northern Paris Basin. Sci. Drilling 3, 138–152.

Deconinck, J.-F., Bernoulli, D., 1991. Clay mineral assemblages of Mesozoic pelagic and flysch sediments of the Lombardian Basin (Southern Alps): implications for palaeotectonics, palaeoclimate and diagenesis. Geol. Rundsch. 80, 1–17.

Deconinck, J.-F., Hesselbo, S.P., Debuisser, N., Averbuch, O., Baudin, F., Bessa, J., 2003. Environmental controls on clay mineralogy of an Early Jurassic mudrock (Blue Lias Formation, southern England). Geol. Rundsch. 92, 255–266.

Delavenna, M.-F., Steinberg, M., Trauth, N., Holtzapffel, T., 1989. Influence des cycles eustatiques et de la tectonique synsédimentaire sur la minéralogie du Lias et du Dogger du forage de Sancerre-Couy (Cher). Programme Géologie profonde de la France. C. R. Acad. Sci. 308, 111–116.

Diekmann, B., Petschick, R., Ginlele, F.X., Fütterer, D.K., Abelmann, A., Brathauer, U., Gersonde, R., Mackensen, A., 1996. Clay minerals fluctuations in Late Quaternary sediments of the southeastern south Atlantic: implications for past changes of deep water advection. In: Wefer, G., Berger, W.H., Siedler, G., Webb, D.J. (Eds.), The South Atlantic: Present and Past Circulation. Springer-Verlag, Berlin Heidelberg, pp. 621–644.

Dommergues, J.-L., Meister, C., Mouterde, R., 1997. Pliensbachien. In: Cariou, E., Hantzpergue, P. (Coord). Biostratigraphie du Jurassique ouest-européen et méditerranéen: zonations parallèles et distribution des invertébrés et microfossiles. Bull. Centre Rech. Explor. Prod. Elf Aquitaine 17, pp. 15–23.

Duarte, L.V., 1998. Clay minerals and geochemical evolution in the Toarcian–Lower Aalenian of the Lusitanian Basin (Portugal). Cuad. Geol. Ibér. 24, 69–98.

Elmi, S., Rulleau, L., Gabilly, J., Mouterde, R., 1997. Toarcien. In: Cariou, E., Hantzpergue, P. (Coord). Biostratigraphie du Jurassique ouest-européen et méditerranéen: zonations parallèles et distribution des invertébrés et microfossiles. Bull. Centre Rech. Explor. Prod. Elf Aquitaine 17, pp. 25–36.

Enay, R., Mangold, C., 1982. Dynamique biogéographique et évolution des faunes d'ammonites du Jurassique. Bull. Soc. Géol. France 7, 1025–1046.

Gibbs, R.J., 1977. Clay-mineral segregation in the marine environment. J. Sediment. Petrol. 47, 237–243.

Gómez, J.J., Goy, A., Canales, M.L., 2008. Seawater temperature and carbon isotope variations in belemnites linked to mass extinction during the Toarcian (Early Jurassic) in Central and Northern Spain. Comparison with other European sections. Palaeogeogr. Palaeoclimatol. Palaeoecol. 258, 28–58.

Goto, M., Tazaki, K., 1998. Clay mineral analysis of the paleo-environment: sedimentary environment of the Kuruma Group. Nendo Kagaku 38, 91–102 (in Japanese, with English Abstr.).

Gradstein, F.M., Ogg, J.G., Smith, A.G., 2004. A Geologic Time Scale 2004. Cambridge University Press, Cambridge.

Hadri, M., 1993. Un modèle de plateforme carbonatée au Lias-Dogger dans le Haut-Atlas central au Nord-Ouest de Goulimina, Maroc. Ph.D. Thesis, Univ. Paris 11, Paris, France.

Hallam, A., Grose, J.A., Ruffell, A.H., 1991. Palaeoclimatic significance of changes in clay mineralogy across the Jurassic–Cretaceous boundary in England and France. Palaeogeogr. Palaeoclimatol. Palaeoecol. 81, 173–187.

Hardenbol, J., Thierry, J., Farley, M.B., de Graciansky, P.-C., Vail, P.R., 1998. Mesozoic and Cenozoic sequence chronostratigraphic framework of European basins. In: de Graciansky, P.-C., Hardenbol, J., Jacquin, T., Vail, P.R. (Eds.), Mesozoic and Cenozoic Sequence Stratigraphy of European basins. Special Publication, Society for Sedimentary Geology, vol. 60, pp. 3–13.

Hesselbo, S.P., Gröcke, D.R., Jenkyns, H.C., Bjerrum, C.J., Farrimond, P., Morgans-Bell, H.S., Green, O.R., 2000a. Massive dissociation of gas hydrates during a Jurassic oceanic anoxic event. Nature 406, 392–395.

Hesselbo, S.P., Meister, C., Gröcke, D.R., 2000b. A potential global stratotype for the Sinemurian–Pliensbachian boundary (Lower Jurassic), Robin Hood's Bay, UK: ammonite faunas and isotope stratigraphy. Geol. Mag. 137, 601–607.

Hesselbo, S.P., Jenkyns, H.C., Duarte, L.V., Oliveira, L.C.V., 2007. Carbon-isotope record of the Early Jurassic (Toarcian) Oceanic Anoxic Event from fossil wood and marine carbonate (Lusitanian Basin, Portugal). Earth Planet. Sci. Lett. 253, 455–470.

Hillier, S., Wilson, M.J., Merriman, R.J., 2006. Clay mineralogy of the Old Red Sandstone and Devonian sedimentary rocks of Wales, Scotland and England. Clay Miner. 41, 433–471.

Hurst, A., 1985a. The implication of clay mineralogy to palaeoclimate and provenance during the Jurassic in NE Scotland. Scot. J. Geol. 21, 143–160.

Hurst, A., 1985b. Mineralogy and diagenesis of Lower Jurassic sediments of the Lossiemouth borehole, north-east Scotland. Proc. Yorks. Geol. Soc. 45, 189–197.

Jamoussi, F., Bédir, M., Boukari, N., Kharbachi, S., Zargouni, F., López-Galindo, A., Paquet, H., 2003. Clay mineralogical distribution and tectono-eustatic control in the Tunisian margin basins. C. R. Acad. Sci. 335, 175–183.

Jeans, C.V., 2006. Clay mineralogy of the Jurassic strata of the British Isles. Clay Miner. 41, 187–307.

Jenkyns, H.C., 1988. The early Toarcian (Jurassic) anoxic event: stratigraphic, sedimentary, and geochemical evidence. Am. J. Sci. 288, 101–151.

Jenkyns, H.C., Clayton, C.J., 1997. Lower Jurassic epicontinental carbonates and mudstones from England and Wales: chemostratigraphic signals and the early Toarcian anoxic event. Sedimentology 44, 687–706.

Jenkyns, H.C., Jones, C.E., Gröcke, D.R., Hesselbo, S.P., Parkinson, D.N., 2002. Chemostratigraphy of the Jurassic system: applications, limitations and implications for palaeoceanography. J. Geol. Soc. 159, 351–378.

Jones, C.E., Jenkyns, H.C., 2001. Seawater strontium isotopes, oceanic anoxic events, and seafloor hydrothermal activity in the Jurassic and Cretaceous. Am. J. Sci. 301, 112–149.

Jones, C.E., Jenkyns, H.C., Hesselbo, S.P., 1994. Strontium isotopes in Early Jurassic seawater. Geochim. Cosmochim. Ac. 58, 1285–1301.

Kemp, D.B., Coe, A.L., Cohen, A.S., Schwark, L., 2005a. Astronomical pacing of methane release in the Early Jurassic period. Nature 437, 396–399.

Kemp, S.J., Merriman, R.J., Bouch, J.E., 2005b. Clay mineral reaction progress—the maturity and burial history of the Lias Group of England and Wales. Clay Miner. 40, 43–61.

Lanson, B., Meunier, A., 1995. La transformation des interstratifiés ordonnés (S ≥ 1) illite-smectite en illite dans les série diagénétiques. État des connaissances et perspectives. Bull. Centre Rech. Explor. Prod. Elf Aquitaine 19, 149–165.

Lanson, B., Beaufort, D., Berger, G., Bauer, A., Cassagnabère, A., Meunier, A., 2002. Authigenic kaolin and illitic minerals during burial diagenesis of sandstones: a review. Clay Miner. 37, 1–22.

Leonowicz, P., 2005. The Ciechocinek Formation (Lower Jurassic) of SW Poland: petrology of green clastic rocks. Geol. Q. 49, 317–330.

Little, C.T.S., Benton, M.J., 1995. Early Jurassic mass extinction: a global long term event. Geology 23, 495–498.

Liu, C., Heinze, M., Fürsich, F.T., 1998. Bivalve provinces in the Proto-Atlantic and along the southern margin of the Tethys in the Jurassic. Palaeogeogr. Palaeoclimatol. Palaeoecol. 137, 127–151.

McArthur, M., Donovan, D.T., Thirlwall, M.F., Fouke, B.W., Mattey, D., 2000. Strontium isotope profile of the early Toarcian (Jurassic) oceanic anoxic event, the duration of ammonite biozones, and belemnite palaeotemperatures. Earth Planet. Sci. Lett. 179, 269–285.

McElwain, J.C., Wade-Murphy, J., Hesselbo, S.P., 2005. Changes in carbon dioxide during an oceanic anoxic event linked to intrusion into Gondwana coals. Nature 435, 479–482.

Metodiev, L., Koleva-Rekalova, E., 2006. Carbon and oxygen isotope record of Lower–Middle Jurassic belemnites and rocks from the Western Balkan Mts (Bulgaria). Volumina Jurassica 4, 7th Int. Congress on the Jurassic System, Kraków, Poland, pp. 188–190.

Monaco, P., Nocchi, M., Ortega-Huertas, M., Palomo, I., Martinez, F., Chiavini, G., 1994. Depositional trends in the Valdorbia Section (Central Italy) during the Early Jurassic, as revealed by micropaleontology, sedimentology and geochemistry. Eclogae geol. Helv. 87, 157–223.

Moore, D.M., Reynolds, R.C., 1997. X-ray Diffraction and the Identification and Analysis of Clay Minerals. Oxford Univ. Press, New York.
Mørk, M.B.E., Vigran, J.O., Smelror, M., Fjerdingstad, V., Bøe, R., 2003. Mesozoic mudstone compositions and the role of kaolinite weathering—a view from shallow cores in the Norwegian Sea (Møre to Troms). Norwegian J. Geol. 83, 61–78.
Mouterde, R., Elmi, S., 1991. Caractères différentiels des faunes d'ammonites du Toarcien des bordures de la Téthys. Signification paléogéographique. Bull. Soc. Géol. France 162, 1185–1195.
Nielsen, O.B., Seidenkrantz, M.-S., Abrahamsen, N., Schmidt, B.J., Koppelhus, E.B., Ravn-Sørensen, H., Korsbech, U., Nielsen, K.G., 2003. The Lower–Middle Jurassic of the Anholt borehole: Implication for the geological evolution of the eastern margin of the Danish Basin. Geol. Surv. Den. Greenl. Bull. 1, 585–609.
Oliveira, L.C.V., Rodrigues, R., Duarte, L.V., Lemos, V.B., 2006. Oil generation potential assessment and paleoenvironmental interpretation based on biomarkers and stable carbon isotopes of the Pliensbachian–Lower Toarcian (Lower Jurassic) of the Peniche region (Lusitanian Basin, Portugal). B. Geoci. Petrobras 14, 207–234.
Ortega-Huertas, M., Monaco, P., Palomo, I., 1993. First data on clay mineral assemblages and geochemical characteristics of Toarcian sedimentation in the Umbria–Marche Basin (Central Italy). Clay Miner. 28, 297–310.
Pálfy, J., Smith, P.L., 2000. Synchrony between Early Jurassic extinction, oceanic anoxic event, and the Karoo-Ferrar flood basalt volcanism. Geology 28, 747–750.
Palomo-Delgado, I., Ortega-Huertas, M., Fenoll-Hach-Ali, P., 1985. The significance of clay minerals in studies of the evolution of the Jurassic deposits of the Betic Cordillera, SE Spain. Clay Miner. 20, 39–52.
Pearson, M.J., 1990. Clay mineral distribution and provenance in Mesozoic and Tertiary mudrocks of the Moray Firth and northern North Sea. Clay Miner. 25, 519–541.
Pellenard, P., Deconinck, J.-F., 2006. Mineralogical variability of Callovo–Oxfordian clays from the Paris Basin and the Subalpine Basin. C. R. Geosci. 338, 854–866.
Raucsik, B., Merény, L., 2000. Origin and environmental significance of clay minerals in the Lower Jurassic formations of the Mecsek Mts, Hungary. Acta Geol. Hungarica 43, 405–429.
Raucsik, B., Varga, A., 2008. Climato-environmental controls on clay mineralogy of the Hettangian–Bajocian successions of the Mecsek Mountains, Hungary: an evidence for extreme continental weathering during the early Toarcian oceanic anoxic event. Palaeogeogr. Palaeoclimatol. Palaeoecol. 265, 1–13.
Rees, P.M., Ziegler, A.M., Valdes, P.J., 2000. Jurassic phytogeography and climates: new data and model comparisons. In: Huber, B.T., Macleod, K.G., Wing, S.L. (Eds.), Warm climates in Earth history. Cambridge University Press, pp. 297–318.
Renac, C., Meunier, A., 1995. Reconstruction of palaeothermal conditions in a passive margin using illite–smectite mixed-layer series (BA1 Scientific Deep Drill-Hole, Ardèche, France). Clay Miner. 30, 107–118.
Rosales, I., Quesada, S., Robles, S., 2004. Paleotemperature variations of Early Jurassic seawater recorded in geochemical trends of belemnites from the Basque–Cantabrian basin, northern Spain. Palaeogeogr. Palaeoclimatol. Palaeoecol. 203, 253–275.
Ruffell, A., McKinley, J.M., Worden, R.H., 2002. Comparison of clay mineral stratigraphy to other proxy palaeoclimate indicators in the Mesozoic of NW Europe. Phil. T. Roy. Soc. A 360, 675–693.
Schnyder, J., Ruffell, A., Deconinck, J.-F., Baudin, F., 2006. Conjunctive use of spectral gamma-ray logs and clay mineralogy in defining late Jurassic–early Cretaceous palaeoclimate change (Dorset, U.K.). Palaeogeogr. Palaeoclimatol. Palaeoecol. 229, 303–320.
Schouten, S., Kaam-Peters, M.E., Rijpstra, I., Schoell, M., Sinnighe Damste, J.S., 2000. Effects of an oceanic anoxic event on the stable carbon isotopic composition of early Toarcian carbon. Am. J. Sci. 300, 1–22.
Shaw, H.F., 2006. Clay mineralogy of Carboniferous sandstone reservoirs, onshore and offshore UK. Clay Miner. 41, 417–432.
Singer, A., 1984. The paleoclimatic interpretation of clay minerals in sediments—a review. Earth-Sci. Rev. 21, 251–293.
Spears, D.A., 2006. Clay mineralogy of onshore UK Carboniferous mudrocks. Clay Miner. 41, 395–416.
Suan, G., Pittet, B., Bour, I., Mattioli, E., Duarte, L.V., Mailliot, S., 2008a. Duration of the Early Toarcian carbon isotope excursion deduced from spectral analysis: consequence for its possible causes. Earth Planet. Sci. Lett. 267, 666–679.
Suan, G., Mattioli, E., Pittet, B., Mailliot, S., Lécuyer, C., 2008b. Evidence for major environmental perturbation prior to and during the Toarcian (Early Jurassic) oceanic anoxic event from the Lusitanian Basin, Portugal. Paleoceanography 23, PA1202. doi:10.1029/2007PA001459.
Svensen, H., Planke, S., Chevallier, L., Malthe-Sørenssen, A., Corfu, F., Jamtveit, B., 2007. Hydrothermal venting of greenhouse gases triggering Early Jurassic global warming. Earth Planet. Sci. Lett. 256, 554–566.
Thierry, J. et al., 2000a. Late Sinemurian. In: Dercourt, J., Gaetani, M., Vrielynck, B., Barrier, E., Biju-Duval, B., Brunet, M.-F., Cadet, J.P., Crasquin, S., Sandulescu, M. (Eds.), Atlas Peri-Tethys Paleogeographical Maps, vol. I–XX.CCGM/CGMW, Paris, map 7, (40 co-authors).
Thierry, J. et al., 2000b. Middle Toarcian. In: Dercourt, J., Gaetani, M., Vrielynck, B., Barrier, E., Biju-Duval, B., Brunet, M.-F., Cadet, J.P., Crasquin, S., Sandulescu, M. (Eds.), Atlas Peri-Tethys Paleogeographical Maps, vol. I–XX.CCGM/CGMW, Paris, map 8, (40 co-authors).
Thiry, M., 2000. Palaeoclimatic interpretation of clay minerals in marine deposits: an outlook from the continental origin. Earth-Sci. Rev. 49, 201–221.
Tremolada, F., Van de Schootbrugge, B., Erba, E., 2005. Early Jurassic schizosphaerellid crisis in Cantabria, Spain: implications for calcification rates and phytoplankton evolution across the Toarcian oceanic anoxic event. Paleoceanography 20, A201. doi:10.1029/2004PA001120.
Uriarte Goti, J.A., 1997. Maturité thermique des sédiments de la bordure sud-est du Bassin de Paris. Ph.D. Thesis, Univ. Genève, Switzerland.
Vanderaveroet, P., Averbuch, O., Deconinck, J.-F., Chamley, H., 1999. A record of glacial/interglacial alternations in Pleistocene sediments of New Jersey expressed by clay mineral, grain-size and magnetic susceptibility data. Mar. Geol. 159, 79–92.
Van de Schootbrugge, B., Bailey, T.R., Rosenthal, Y., Katz, M.E., Wright, J.D., Miller, K.G., Feist-Burkhardt, S., Falkowski, P.G., 2005a. Early Jurassic climate change and the radiation of organic-walled phytoplankton in the Tethys Ocean. Paleobiology 31, 73–97.
Van de Schootbrugge, B., McArthur, J.M., Bailey, T.R., Rosenthal, Y., Wright, J.D., Miller, K.G., 2005b. Toarcian anoxic event: an assessment of global causes using belemnite C isotope records. Paleoceanography 21, PA3008. doi:10.1029/2004PA001102.
Viczián, I., 1995. Clay mineralogy of Jurassic carbonate rocks, Central Transdanubia, Hungary. Acta Geol. Hung. 38, 251–268.
Wignall, P.B., Newton, R.J., Little, C.T.S., 2005. The timing of paleoenvironmental change and cause-and-effect relationships during the early Jurassic mass extinction in Europe. Am. J. Sci. 305, 1014–1032.
Wignall, P.B., McArthur, J.M., Little, C.T.S., Hallam, A., 2006. Palaeoceanography: methane release in the Early Jurassic period. Nature 441. doi:10.1038/nature04905.